MOLECULAR AND CELLULAR BIOLOGY, June 1996, p. 2656–2669 Vol. 16, No. 6
0270-7306/96/$04.00+0

Multiple Single-Stranded *cis* Elements Are Associated with Activated Chromatin of the Human c-*myc* Gene In Vivo

GREGORY A. MICHELOTTI,[1] EMIL F. MICHELOTTI,[1] ANDREA PULLNER,[2] ROBERT C. DUNCAN,[1]† DIRK EICK,[2] AND DAVID LEVENS[1]*

Laboratory of Pathology, National Cancer Institute, Bethesda, Maryland 20892,[1] and Institut für Klinische Molekularbiologie und Tumorgenetik, Forschungszentrum für Umwelt und Gesundheit, D-81377 Munich, Germany[2]

Received 17 November 1995/Returned for modification 4 January 1996/Accepted 1 March 1996

Transcription activation and repression of eukaryotic genes are associated with conformational and topological changes of the DNA and chromatin, altering the spectrum of proteins associated with an active gene. Segments of the human c-*myc* gene possessing non-B structure in vivo were located with enzymatic and chemical probes. Sites hypersensitive to cleavage with the single-strand-specific S1 nuclease or the single-strand-selective agent potassium permanganate included the major promoters P1 and P2 as well as the far upstream sequence element (FUSE) and CT elements, which bind, respectively, the single-strand-specific factors FUSE-binding protein and heterogeneous nuclear ribonucleoprotein K in vitro. Active and inactive c-*myc* genes yielded different patterns of S1 nuclease and permanganate sensitivity, indicating alternative chromatin configurations of active and silent genes. The melting of specific *cis* elements of active c-*myc* genes in vivo suggested that transcriptionally associated torsional strain might assist strand separation and facilitate factor binding. Therefore, the interaction of FUSE-binding protein and heterogeneous nuclear ribonucleoprotein K with supercoiled DNA was studied. Remarkably, both proteins recognize their respective elements torsionally strained but not as linear duplexes. Single-strand- or supercoil-dependent gene regulatory proteins may directly link alterations in DNA conformation and topology with changes in gene expression.

Growing evidence suggests that regulatory DNA is not a static matrix but in fact suffers torsional and flexural stress and strain as molecules interact, translocate, rotate, and writhe during the process of transcription (39). Prokaryotic systems and in vitro model systems constructed from prokaryotic components have been used to demonstrate that distortion of the double helix during transcription leads to local and global changes in DNA conformation. Hairpin extrusion, DNA melting, Z-DNA formation, and supercoiling have all been shown to be consequences of topological strain (14, 39, 67). Several processes which oppose or accommodate these B-DNA disruptive forces have evolved; such processes involve topoisomerases, nucleosomes, matrix attachment proteins, and single-stranded DNA-binding proteins (24). The in vivo steady-state balance between B-DNA, unusual DNA structures, and transcription remains to be explored. Although transcriptionally generated torsion may be a molecular waste product, to be dissipated or disposed of, it is also conceivable that mechanisms exist to measure and harvest energy or information stored in these altered configurations. Several observations suggest that such mechanisms may operate on the c-*myc* gene.

The c-*myc* proto-oncogene, encoding a b-ZIP helix-loop-helix transcription factor and a key regulator of cell growth, differentiation, and death, is controlled by numerous hormones, growth factors, pharmacologic agents, and biological conditions (52, 56; for reviews, see references 34 and 40). No simple pattern describes the response of the c-*myc* gene to multiple signals, nor has a satisfying model emerged to suggest how these multiple signals converge and are integrated to set the levels of c-*myc* expression (16, 57, 58). Many specific interactions have been identified, both in vivo and in vitro, between a host of proteins and a bewildering array of c-*myc* DNA sequences. In addition to conventional transcription factors bearing DNA binding and effector domains (12, 20, 31, 41, 45, 61, 70), several sequence-specific, single-stranded-DNA-binding proteins have been suggested to regulate c-*myc* expression through upstream sequences. These include far upstream sequence element (FUSE)-binding protein (FBP), heterogeneous nuclear ribonucleoprotein (hnRNP) K, cellular nucleic acid-binding protein (CNBP), pur1, MSSP-1, and MSSP-2 (9, 10, 18, 41, 42, 60, 62, 64). The proposed action of these proteins appears to require melting of c-*myc* regulatory elements, thereby coupling this action to DNA conformation. Reports of analyses of c-*myc* single-stranded DNA and Z-DNA in vivo, as well as perturbation of c-*myc* expression by topoisomerase inhibitors, evoke the notion that DNA topology and conformation may help to govern c-*myc* expression (1, 4, 46, 67). Indicative of alterations in chromatin, changes in DNase I hypersensitivity within and flanking the c-*myc* gene have correlated the physical state of the c-*myc* gene with its expression (6, 22, 54). The intensity of cleavage at some sites parallels the synthesis of c-*myc* RNA, whereas other sites are constitutive (6, 7, 51, 53, 54). Although hypersensitivity at the P1 and P2 promoters almost certainly reflects the presence of bound RNA polymerase (68), at the remaining hypersensitive sites, neither the configuration of the DNA nor the identities of the associated factors have been established.

FUSE and the CT region, at positions −1500 and −100, respectively, upstream of the human c-*myc* gene, are *cis* elements which increase c-*myc* promoter activity in transfection assays (3, 61). Biochemical studies to identify the factors recognizing these elements have yielded the sequence-specific single-stranded DNA-binding proteins FBP as well as hnRNP K and CNBP, which recognize opposite strands of the CT element (18, 41, 62). Coexpression of these proteins with reporters either possessing or lacking the appropriate *cis* element

* Corresponding author. Phone: (301) 496-2176. Fax: (301) 402-0043.

† Present address: Laboratory of Molecular Pharmacology, Food and Drug Administration/Center for Biologics Evaluation and Research, Bethesda, MD 20892.

has demonstrated their ability to augment specific gene expression. If c-*myc* expression is regulated by these and other single-stranded-DNA-binding proteins, then some c-*myc cis* elements must assume single-stranded conformation in vivo. Although previous studies have revealed sites sensitive to the single-strand-specific nuclease S1 in the chromatin associated with some promoter regions (30, 38), neither the molecules nor the mechanisms generating S1 sensitivity in vivo have been elucidated. A reliable chemical approach to assess the conformational state of promoters in vivo has been developed (29, 50). The present work applies similar enzymatic and chemical probes to analyze the human c-*myc* promoters and upstream sequences associated with sequence-specific single-stranded-DNA-binding proteins. To determine the particular molecules and mechanisms associated with melting in upstream sequences, the relationship between specific factor binding, transcription, and topology was explored in vivo and in vitro. The ramifications of regulatory factors which could directly affect transcription, conformation, and topology are discussed.

MATERIALS AND METHODS

Cell culture. Stock cultures of HL60, HeLa, U937, and IMR32 cells were grown according to American Type Culture Collection specifications. All cells were maintained in either 100-ml monolayer cultures in T-175 flasks or 500-ml spinner cultures in the appropriate media. HL60, U937, RF266C3, and MA76 cells were grown in RPMI supplemented with 10% (vol/vol) fetal calf serum. HeLa and IMR32 cells were grown in Eagle's minimal essential medium supplemented with 10% (vol/vol) fetal calf serum. Cell densities were kept below 10^6/ml.

DNase I treatment of isolated nuclei. Nuclei were isolated as described previously (54), with the following modifications. After cell disruption in nuclear isolation buffer [300 mM sucrose, 15 mM NaCl, 60 mM KCl, 5 mM $MgCl_2$, 20 mM Tris-HCl (pH 7.8), 1 mM ethylene glycol-bis(β-aminoethyl ether)-*N*,*N*,*N*′,*N*′-tetraacetic acid (EGTA), 1 mM dithiothreitol (DTT), 0.5 mM phenylmethylsulfonyl fluoride] supplemented with 0.2% Nonidet P-40, nuclei were washed several times in cold nuclear isolation buffer. Nuclei were resuspended at 4×10^7/ml in cold nuclear isolation buffer supplemented with 5% glycerol and placed in tubes in 500-μl aliquots. Samples then received the indicated amounts of DNase I (Worthington), each added in a 20-μl aliquot of 100 mM $CaCl_2$–20 mM $MgCl_2$. Nuclei were digested and DNA was purified as described previously (54).

S1 nuclease treatment of isolated nuclei. Isolated nuclei were prepared as described above. After cell disruption, nuclei were washed in cold phosphate-buffered saline (PBS) and washed three times in cold S1 nuclease digestion buffer (30 mM sodium acetate, 3 mM $ZnCl_2$, 1 mM EDTA [pH 4.5]). Nuclei were then resuspended at a concentration of 4×10^7/ml in S1 nuclease digestion buffer prewarmed to 37°C and placed in tubes in 500-μl aliquots. The indicated amount of S1 nuclease (Boehringer Mannheim), or Tris-EDTA for the 0-U control, was added, and samples were digested for 30 min at 37°C. DNA was purified as described above.

Southern blot analysis. Purified DNase I- or S1 nuclease-treated genomic DNA was digested with *Hin*dIII and *Sst*I (New England Biolabs) as recommended by the supplier. To adjust for the amplified c-*myc* copy number in HL60 cells, 2 μg of HL60 DNA and 20 μg of IMR32 DNA were used in restriction digestions. Southern analysis was performed as described previously (2), using a 610-bp *Rsr*II-*Sst*I gel-purified c-*myc* genomic restriction fragment specific for intron I as the probe. The fragment was random-prime labeled by using a Gibco-BRL random-prime labeling kit and [α-^{32}P]dCTP (6,000 Ci/mmol; New England Nuclear) to a specific activity of $>10^9$ cpm/μg. Approximately 10^7 cpm of probe per ml was added to the prehybridization buffer, and blots were hybridized overnight at 42°C. Blots were washed in 0.5× SSC (1× SSC is 0.15 M NaCl plus 0.015 sodium citrate)–1% sodium dodecyl sulfate (SDS) at 65°C and exposed to either Kodak XAR-5 or BIOMAX film for autoradiography.

Protein expression and electrophoretic mobility shift assays. Recombinant protein was purified from extracts of *Escherichia coli* transformed with plasmid pGEX-FBP, pGEX-FBP_{3+4}, pGEX-FBP_{1+2}, pGEX-hnRNP K, or pGEX-CNBP on a glutathione-agarose matrix (Sigma). Sp1 was purchased from Promega. Glutathione *S*-transferase (GST) was purified from cells carrying plasmid pGEX-2T with no insert. Recombinant proteins were eluted from glutathione beads in 20 mM glutathione and checked by SDS-polyacrylamide gel electrophoresis for purity, correct size, and concentration. Construct pGEX-FBP_{1+2} contains an FBP fragment specific for residues 103 to 267 of the full-length protein. Construct pGEX-FBP_{3+4} contains an FBP fragment specific for residues 278 to 474 of the full-length protein.

Electrophoretic mobility shift assays were performed as described previously (18), with the following modifications. The indicated recombinant protein and labeled probe (0.05 ng) were incubated in 10 μl of binding buffer [20 mM *N*-2-hydroxyethylpiperazine-*N*′-2-ethanesulfonic acid (HEPES; pH 8.0), 100 mM NaCl, 1 mg of bovine serum albumin (BSA) per ml, 5% glycerol, 1 mM DTT, 10 ng of poly(dI-dC) per ml] for 30 min at 0°C. Probes were prepared by 5′ end labeling synthetic oligonucleotides with T4 DNA kinase in the presence of [γ-^{32}P]ATP, and the two probes were adjusted to the same specific activity. After the binding reaction, samples were resolved on an 8% native polyacrylamide gel and run at 4°C. The 3′ FUSE noncoding-strand oligonucleotide was 5′-GATCCTATATTC CCTCGGGATTTTTTATTTTGT-3′, encompassing positions −1554 to −1525; the 5′ FUSE noncoding-strand oligonucleotide was 5′-GATCTTTTTTATTTTGTGT TATTCCACGGCATGAAAAACAA-3′, corresponding to positions −1577 to −1541 of c-*myc*. Nonspecific oligonucleotide 1, used as competitor with the 3′ probe, was 5′-AATTCTCCTCCCCACCTTCCCCACCCCTCCCCA-3′, corresponding to the top strand of the CT region (−153 to −116), relative to P1. Nonspecific oligonucleotide 2, used as a competitor with the 5′ probe, was 5′-GGCCGAATTACTA CAGCGAGTTAGATAAAGCCCCGAAAACCGGGTTTTATACCTTC-3′, corresponding to a modified segment of the bottom strand of the P2 region from +178 to 131, relative to P1.

TABLE 1. Primer sets for LMPCR

Primers for:	Sequences
FUSE top strand	(−1448) CGCTTCGACTCAGCTAGTTGC (−1468)
	ACTCAGCTAGTTGCCCAGCCCCA
	GCTAGTTGCCCAGCCCCACACATGAT
FUSE bottom strand	(−1654) TTTGGAGGTGGTGGAGGGAG (−1635)
	GAGGTGGTGGAGGGAGAGAAAAG
	GGTGGAGGGAGAGAAAAGTTTACTTAAAATGCC
CT top strand	(−9) GTCCAGACCCTCGCATT (−25)
	AGACCCTCGCATTATAAAGGGCC
	GCATTATAAAGGGCCGGTGGGCGGAG
CT bottom strand	(−234) GGTAGGCGCGCGTAGTT (−218)
	GGCGCGCGTAGTTAATTCATGCG
	GCGCGTAGTTATTCATGCGGCTCTC
P2 bottom strand	(+94) TTGGCGGGAAAAAGAAC (+110)
	GGCGGGAAAAAGAACGGAGGGAG
	AAAGAACGGAGGGAGGGATCGCGCTG

In vivo and in vitro $KMnO_4$ treatment and DNA isolation. Potassium permanganate ($KMnO_4$) modification of whole cells and naked genomic DNA samples was performed exactly as described previously (18). For plasmid reactions, recombinant protein (0.4 to 4 μg) was incubated with 10 ng of either supercoiled or *Hin*dIII-linearized plasmid DNA. The plasmid was a 3.3-kb *Hin*dIII-*Sst*I genomic c-*myc* fragment cloned into a pUC derivative and has been described in detail elsewhere (18). Recombinant proteins were all GST fusion proteins prepared as described above, except for Sp1, which was obtained from Promega. Plasmid DNA was incubated with the appropriate recombinant protein in 60 μl of binding buffer (20 mM HEPES [pH 8.0], 5 mM NaCl, 100 μg of BSA per ml, 0.5 mM EDTA, 1 mM DTT) for 15 min at room temperature. Reaction mixtures for Sp1, hnRNP K, and CNBP were also supplemented with 50 μM $ZnCl_2$. $KMnO_4$ was added for 30 s on ice to a final concentration of 25 mM, and reactions were stopped by addition of an equal volume of stop buffer lacking SDS. Modified DNA was cleaved with piperidine and purified as described above, with the modification that carrier tRNA was added to a final concentration of 100 μg/ml. DNA was resuspended in Tris-EDTA, and 100 pg was used for ligation-mediated PCR (LMPCR).

LMPCR. LMPCR was performed by the method of Garrity and Wold (26), with the following modifications. To 3 μg (5 μl) of DNA was added 25 μl of a 1.2× master mix (12 mM Tris-HCl [pH 8.8], 48 mM NaCl, 6 mM $MgCl_2$, 0.012% BSA, 240 μM each nucleoside triphosphate, 2 pmol of gene-specific primer 1, 0.5 U of Vent DNA polymerase [New England Biolabs]). Following the initial primer extension step, reactions were extracted with phenol-chloroform (1:1) and subjected to ethanol precipitation in 2.5 M ammonium acetate. Samples were resuspended in 75 μl of ligation solution (50 mM Tris-HCl [pH 7.6], 10 mM $MgCl_2$, 3 mM ATP, 1 mM DTT, 5% polyethylene glycol 8000, 100 pmol of unidirectional linker, 3 U of T4 DNA ligase [Boehringer Mannheim]) and incubated for 4 h at room temperature. After the labeling step, samples were extracted with phenol-chloroform (1:1), ethanol precipitated, dried, and resuspended in formamide loading dye. Equal numbers of counts were loaded onto either 6 or 8% sequencing gels and visualized by autoradiography.

Primer sets for LMPCR. See Table 1.

Mapping of nucleosomes. Nuclei were isolated essentially according to a nuclear run-on protocol (23). A total of 2×10^7 nuclei in 200 μl of buffer (30 mM Tris-HCl [pH 8.3], 150 mM KCl, 10 mM $CaCl_2$, 5 mM $MgCl_2$, 20% glycerol, 0.05 mM EDTA) were incubated for increasing periods of times with 3 U of micrococcal nuclease (Sigma, Deisenhofen, Germany). The reaction was stopped by the addition of 10 μl of 0.5 M EDTA. DNA was purified and cut with the indicated restriction enzymes. DNA fragments were separated in a 2% agarose gel, transferred to a nylon membrane, and hybridized with multiprime-labeled PCR probes as described previously (48). DNA probes were generated by PCR,

using specific primers of the c-*myc* gene locus. The following primer pairs were used (primer positions refer to the sequence of Gazin et al. [27] and are given in the order sense-antisense): probe 1, 242 to 265-292 to 315; probe 2, 830 to 853-1153 to 1177; and probe 3, 1153 to 1177-1343 to 1367. PCR fragments were multiprime labeled with [α-^{32}P]CTP.

RESULTS

DNase I and S1 nuclease sites colocalize in the chromatin of the human c-*myc* gene. If single-stranded-DNA-binding proteins help to regulate c-*myc* expression, then some c-*myc* *cis* elements should display single-stranded character in vivo. To identify candidate single-stranded regions of the c-*myc* gene, nuclei from HL60 promonomyelocytic leukemia cells containing an amplified copy of the c-*myc* gene and overexpressing c-*myc* were isolated and treated with single-strand-specific S1 nuclease (66). S1-hypersensitive sites were revealed by Southern blot analysis and indirect end labeling (Fig. 1) (69). Because of the breadth of the hypersensitive sites, and because both strands must be cleaved to generate a band, S1 sensitivity may result from localized melting of a DNA segment.

The patterns of S1 and DNase I sensitivity were directly compared to determine if they were manifestations of similar phenomena. The locations of DNase I-hypersensitive sites I, II_1, II_2, III_1, and III_2 were confirmed (Fig. 1, lane 2). Every DNase I-hypersensitive site was also an S1-hypersensitive site (Fig. 1; compare lanes 2 and 6). (Note that the diffuse morphology of S1 nuclease sensitivity in the II_1 region might indicate conformational changes detected better with S1 nuclease than with DNase I. Accordingly, we refer to this zone as site II_0-II_{1a} to emphasize a distinction in specificity between S1 nuclease and DNase I.) Another S1-sensitive site in the same vicinity was designated II_{1s}. Most of the S1 nuclease and DNase I hypersensitivities corresponded roughly with sequences defined as candidate *cis* elements through the binding in vitro of sequence-specific single-stranded-DNA-binding proteins, including MSSP-1, MSSP-2, FUSE, and the CT element, as well as promoters P1 and P2 (Fig. 1). Hypersensitive site II_2, though regulated and intense, has been less well characterized (55).

DNase I hypersensitivity at some sites is coregulated with c-*myc* expression (21, 54). To determine if S1 nuclease hypersensitivity was also related to c-*myc* expression, we compared the digestion patterns of c-*myc*-expressing HL60 leukemia cells and c-*myc*-repressed, N-*myc*-amplified IMR32 neuroblastoma cells. The previous observation that IMR32 cells are completely devoid of c-*myc* message was confirmed (Fig. 1, inset). Moreover, the c-*myc* alleles are neither amplified nor rearranged; therefore, cell line IMR32 is an excellent model with which to study c-*myc* repression (25, 35). The c-*myc* chromatin structure differed between the leukemia and neuroblastoma cells. Two HL60 S1-hypersensitive sites (II_0-II_{1a} and II_{1s}; also seen in U937 cells [data not shown]) are lost in IMR32 cells; one (site II_0-II_{1a}) corresponds approximately to the location of FUSE (Fig. 1, lanes 7 and 8). The association of S1 nuclease with DNase I hypersensitivity may be more general, as similar observations have been reported for the chicken globin gene, in which S1 and DNase I nuclease-hypersensitive sites colocalize and correlate with globin expression (38). The similar patterns of DNase I and S1 digestion, despite different pH optima, indicate that hypersensitivity to the latter is not due to exposure of nuclei to pH 4.5.

Nucleosome structure at FUSE is disrupted in cells with an activated c-*myc*. Specific sites upstream of c-*myc* become susceptible to cleavage by S1 nuclease or DNase I when the gene is expressed. To determine if the nucleosome array along the c-*myc* gene might be similarly perturbed with expression, the chromatin structures of the c-*myc* genes in two closely related and well-characterized B-cell lines were compared (59). Both cell lines carry ~30 episomal copies of a stably transfected human c-*myc* gene. In the first line, RF266C3, c-*myc* has been placed adjacent to the κ-3′ enhancer, allowing c-*myc* expression after stimulation with sodium butyrate. The c-*myc* construct in MA76 cells lacks the κ-3′ enhancer and fails to express c-*myc*, even after treatment with sodium butyrate (59). Many features of c-*myc* nucleosomal architecture are shared by these two cell lines. For example, hybridization with probe 1 (Fig. 2H) revealed a ladder after micrococcal nuclease digestion (Fig. 2A and B, lanes 5). In both cell lines, cleavage with *Hin*dIII truncated the nucleosomal ladder after two steps (Fig.

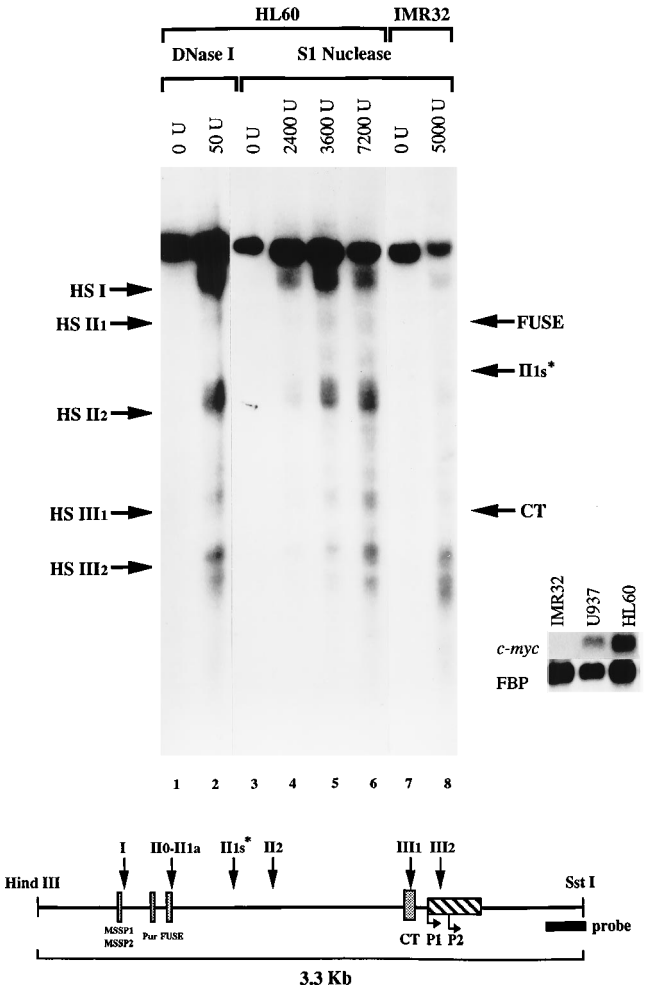

FIG. 1. Comparison of DNase I and S1 nuclease sensitivities in the 5′ regulatory regions of human c-*myc* in HL60 and IMR32 cells. Isolated nuclei were treated with increasing amounts of either DNase I or S1 nuclease. DNA was then purified, digested with *Hin*dIII and *Sst*I, fractionated on a 1% agarose gel, transferred to a nylon membrane, and probed with an *Rsr*II-*Sst*I c-*myc* fragment specific for intron I. To normalize for c-*myc* copy number, 2 μg of HL60 DNA and 20 μg of IMR32 DNA were loaded. The locations of DNase I-hypersensitive (HS) I to III_2 as well as the FUSE and CT regions were assigned by reference to *Hae*III fragments of ϕX DNA and *Hin*dIII fragments of λ DNA, which were used as molecular weight markers (not shown). These sites are schematically represented at the bottom. Additionally, S1 nuclease sites II_0-II_{1a} and II_{1s} are designated and explained in further detail in the text. The asterisk by site II_{1s} indicates that it is specific for S1 nuclease. (Inset) IMR32 cells produce FBP but no c-*myc* mRNA. IMR32, HL60, and U937 total RNAs were purified, size fractionated on a formaldehyde-agarose gel, transferred to nitrocellulose, and probed successively with the indicated cDNA probes.

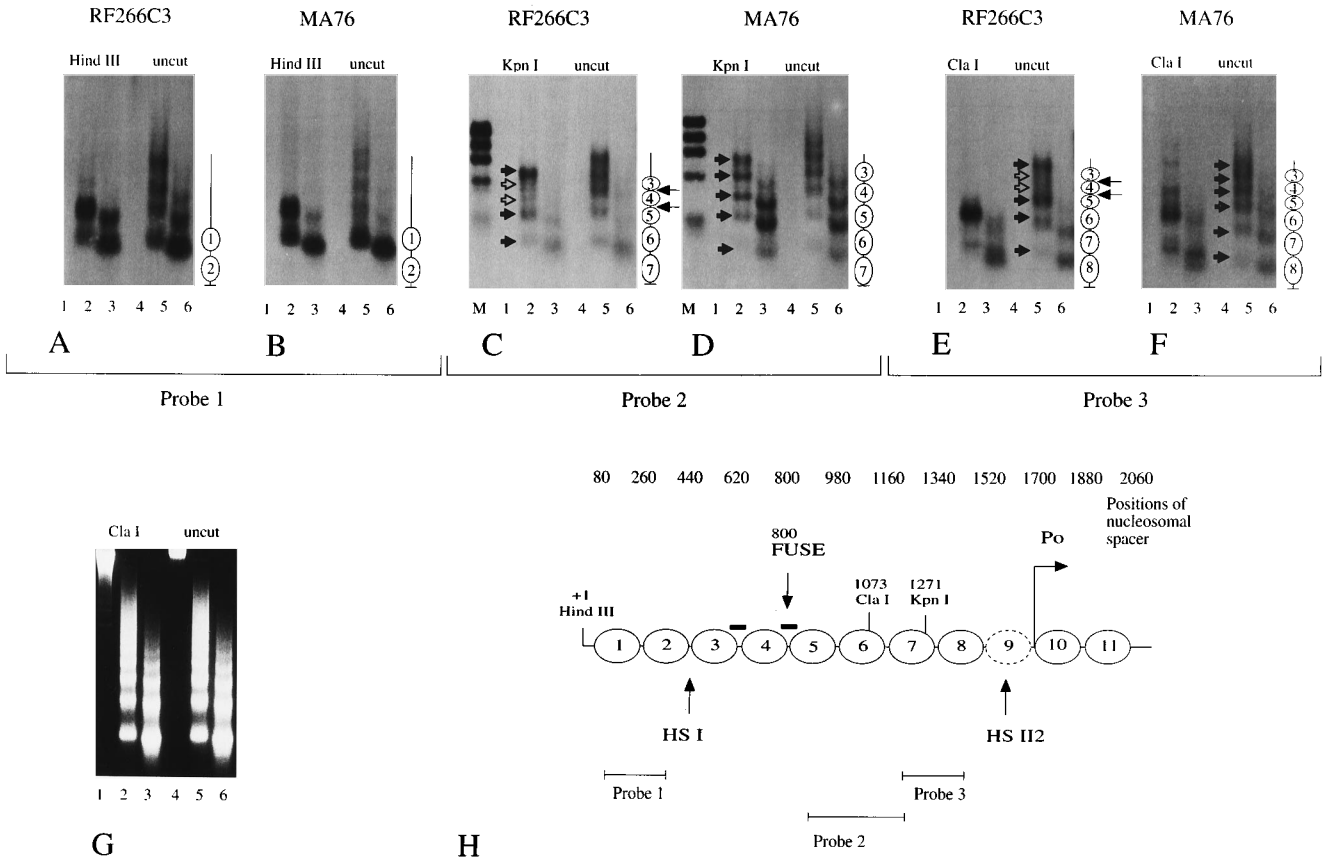

FIG. 2. Nucleosomal structure of the c-*myc* P2 promoter upstream region. Chromatin of RF266C3 and MA76 nuclei was cut to various extents with micrococcal nuclease. DNA was purified, cut with the indicated restriction enzymes (lanes 1 to 3), separated on a 2% agarose gel, transferred to a nylon membrane, and hybridized with probe 1 (A and B), probe 2 (C and D), and probe 3 (E and F). Probes are PCR fragments labeled by multiprime reaction. (G) Ethidium bromide-stained gel before transfer. (H) Map depicting the positions of nucleosomes. M, marker fragments.

2A and B, lanes 2). Therefore, the nucleosomes removed map upstream of the *Hin*dIII site. The lack of visualization of more than two nucleosomes downstream of the *Hin*dIII site, using probe 1, was due to complete micrococcal nuclease cutting at hypersensitive site I (position 440 [Fig. 2H]).

In contrast, hybridization with probe 2 revealed a remarkable difference in micrococcal nuclease sensitivity between the cells capable of expressing c-*myc* (RF266C3) and those in which c-*myc* was silent (MA76). Cleavage of the DNA with *Kpn*I and subsequent hybridization with probe 2 detected five evenly spaced nucleosomes in MA76 cells (Fig. 2D, lane 2) but only three in RF266C3 cells because of lack of cleavage between nucleosomes 3 and 5 (Fig. 2C, lane 2). The disrupted chromatin in RF266C3 encompassed the FUSE region.

The resistance of the region between nucleosomes 3 and 5 to micrococcal nuclease in RF266C3 cells was confirmed by hybridization with probe 3. A regular ladder of six nucleosomes was detected by this probe in MA76 cells (Fig. 2F, lane 5). Because digestion with *Cla*I removed nucleosomes 3 through 6, this restriction site must lie between the probe and the nucleosomes removed. Again, in the nuclei of RF266C3 cells, micrococcal nuclease cutting was blocked between nucleosomes 3 and 5. Once again, the relevant hybridizations were eliminated by *Cla*I digestion, thus mapping the altered chromatin to the FUSE region. With both cell lines, the residual chromatin ladder visualized after cutting with *Cla*I terminated in the vicinity of DNase I-hypersensitive site II_2. This region was almost quantitatively sensitive to micrococcal nuclease in RF266C3 cells (Fig. 2E, lane 2) but was partially resistant in MA76 cells (Fig. 2F, lane 2). These data indicate the existence of a peculiar chromatin structure between nucleosomes 3 and 5 in cells carrying c-*myc* adjacent to the κ-3′ enhancer. The correlation between altered sensitivity of discrete segments of c-*myc* chromatin to nuclease cleavage and c-*myc* expression required further investigation with more sensitive and precise methods to examine the structures of specific *cis* elements.

FUSE is melted only in cells which express c-*myc*. Are S1 nuclease-hypersensitive sites locally melted DNA complexed with protein (perhaps specific *trans* factors), or do they result from some other DNA perturbation? Several sequence-specific single-stranded DNA-binding proteins have been shown to interact with the c-*myc* upstream sequence in vitro. These proteins include FBP (which binds to FUSE) and hnRNP K and CNBP (which bind to the top and bottom strands of the CT element, respectively). If these proteins bind to their respective *cis* elements as single strands in vivo, this altered conformation should react with potassium permanganate. The fine structure of each of these elements was examined by potassium permanganate modification linked to LMPCR (Materials and Methods). Potassium permanganate, which preferentially oxidizes unpaired thymines, has emerged as an important tool with which to analyze open or altered DNA conformations (29, 43, 50). DNA is subsequently cleaved at the modified residues with piperidine followed by visualization of the strand

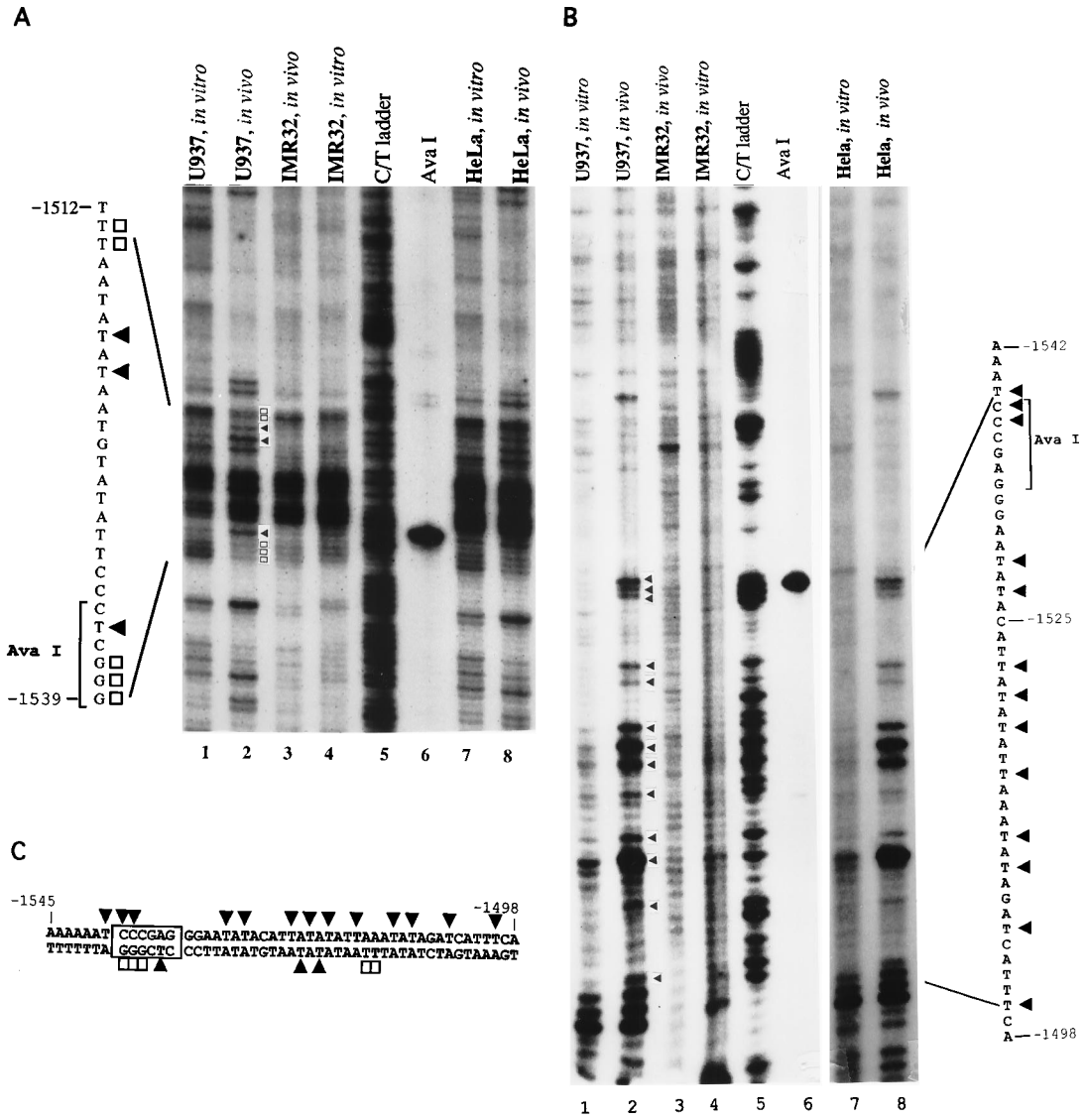

FIG. 3. FUSE is melted only in cells which express c-*myc*. (A) The bottom strand of FUSE is undisturbed in vivo in cells not expressing c-*myc*. Log-phase U937 and HeLa cells (which express c-*myc*) or IMR32 cells (which do not express c-*myc*) as well as naked genomic DNA were treated with 25 mM $KMnO_4$ for 30 s at 0°C. DNA was then purified and treated with piperidine to cleave at the modified bases. Strand breaks were visualized by LMPCR with FUSE bottom-strand primers (Materials and Methods). Pyrimidine ladders were generated by hydrazine modification of human c-*myc* DNA followed by piperidine treatment and LMPCR (47). The *Ava*I site was displayed by cleavage with *Ava*I followed by LMPCR. Hyperreactive residues are marked by triangles; hyporeactive residues are marked by squares. Numbering is relative to P1. (B) $KMnO_4$ reactivity on the FUSE bottom strand in vivo correlates with c-*myc* expression. Reactions were prepared and run as described for panel A, with FUSE top-strand primers. Hypersensitivities in U937 and HeLa chromatin relative to naked genomic DNA are indicated by triangles. (C) Sequence summary of $KMnO_4$ modifications to FUSE. Designations are identical to those described above. The *Ava*I site is boxed and shown for reference.

breaks by LMPCR, thus providing analysis of chromatin structure with single-nucleotide resolution. For these studies, a cell line with one c-*myc* gene per genome was studied to avoid complications due to the potential for microheterogeneity in the promoter of the repeated copies in HL60 cells. Additionally, the sensitivity of PCR obviates any advantage of elevated copy number exploited for Southern blot analysis. Therefore, subsequent experiments were performed with U937 monocytic leukemia cells in addition to IMR32 neuroblastoma cells, both of which contain the c-*myc* locus as a single unrearranged copy per haploid genome.

Proliferating cells or naked genomic DNA was treated with $KMnO_4$ in vivo or in vitro, respectively, and the modified bases were mapped and compared with reference pyrimidine (C+T) or purine (A+G) ladders. The bottom strand (the noncoding or template strand for a c-*myc* transcript) of FUSE displays both hyporeactive and hyperreactive bases in cells that express c-*myc* (Fig. 3A, lanes 1, 2, 7, and 8). The same in vivo pattern was present in HeLa cells, in which c-*myc* expression is high and the c-*myc* gene is present as a single copy (Fig. 3A, lanes 7 and 8), including the protection of three guanine residues (−1537, −1538, and −1539) that are reactive in naked DNA. This unusual but not unprecedented $KMnO_4$ modification of guanines may be due to an altered conformation at this site (18, 28). Other changes that are common to both U937 and HeLa cells are summarized at the left of Fig. 3A and in Fig. 3C. In vitro, FBP binds only to the bottom strand and shows no affinity for the top strand, consistent with the $KMnO_4$ reactivity

of FUSE in vivo (18). None of the $KMnO_4$-induced changes seen in either U937 or HeLa cells are present in IMR32 cells. In fact, with minor exceptions, the in vivo pattern of base modifications in IMR32 cells is identical with that of naked, genomic DNA (Fig. 3A, lanes 3 and 4).

The top strand (the coding strand or the same strand as an RNA transcript) of the FUSE site in U937 in vivo displays increased $KMnO_4$ reactivity compared with purified genomic DNA (Fig. 3B, lanes 1 and 2). U937 and HeLa samples display similar $KMnO_4$ in vivo footprints (Fig. 3B, lanes 7 and 8). These hypersensitivities correspond to thymines at −1540, −1529, −1527, −1522, −1520, −1518, −1515, −1511, −1509, −1505, and −1500 and cytosines at −1539 and −1538, relative to P1. In contrast, the oxidation pattern of the FUSE region in IMR32 cells, lacking c-*myc* RNA, was almost indistinguishable from that of naked DNA (Fig. 3B, lanes 3 and 4). Changes are summarized in Fig. 3C. Taken together, these data suggest a mechanism relating open c-*myc* chromatin structure, single-stranded features at the FUSE site, and c-*myc* expression.

Why was the FUSE in a duplex form in IMR32 neuroblastoma cells? Either the factors which bind and stabilize single-stranded FUSE are missing in IMR32 or these factors are present but the FUSE site is locked in a configuration that is incompatible with single-strand-recognizing proteins. As strong evidence suggests that FBP mediates FUSE function in vivo (18), electrophoretic mobility shift assays and Northern (RNA) analysis were performed with IMR32 whole-cell extracts and RNA, respectively, to determine if the vacancy of the FUSE site is due to the lack of FBP. Indeed, IMR32 cells express both FBP mRNA and FBP which bound to FUSE in vitro (Fig. 1, inset, and data not shown); therefore, if FBP mediates FUSE activity, then either FUSE or FBP must be rendered incompetent to interact with the other in IMR32 (see below).

Repressed c-*myc* promoters adopt a novel conformation. The sensitivity of P1 and P2 to S1 nuclease in neuroblastoma cells suggested that these promoters are not duplex. If an arrested elongation complex is responsible for c-*myc* repression in neuroblastoma cells, then the pattern of $KMnO_4$ reactivity in these cells should resemble that seen in cells which express c-*myc*. Alternatively, a distinct $KMnO_4$ profile would indicate that other mechanisms contribute to c-*myc* repression in IMR32 cells. The in vivo $KMnO_4$ reactions with P1 in IMR32 cells indicated that the region is unwound or distorted but distinct from P1 in U937 cells. On the bottom (template) strand, a number of cleavages were seen in U937 cells, mapping to thymines −25, −19, −10, −3, +1, and +8 as well as cytosine −17, relative to the RNA start site at P1 (Fig. 4A, lanes 1 and 2). None of these changes were detected in neuroblastoma cells (lanes 3 and 4), but a pattern distinct from either that of U937 cells or naked DNA was generated (summarized in Fig. 4C).

To determine whether the differences between repressed and activated c-*myc* genes were manifested at both promoters, similar experiments characterized P2 and generated equivalent results. The pattern of reactivity in U937 cells was almost identical to that reported for HL60 (37). (The greater hypersensitivity in U937 than in HL60 of thymines +14, +15, +20, +32, and +62, relative to P2, most likely reflects increased resolution due to utilization of primers closer to P2.) These data highlighting the differences between neuroblastoma and U937 cells are summarized in Fig. 4C. The top (coding) strand was not studied because of a lack of thymine residues in this region. Thus, the two cell lines exhibit very different underwound structures at the promoter sites. It appears that three states of the major c-*myc* promoters exist: active, repressed, and unoccupied. The last state, while not seen in this study, was noted previously following prolonged differentiation of HL60 cells (37).

Sequence-specific single-stranded-DNA-binding proteins target and melt the FUSE and CT regions in supercoiled DNA. The results described above indicated that several discrete segments of unwound or distorted DNA occur at defined sites in the c-*myc* gene. At promoters complexed with active or stalled RNA polymerase, this result is expected. More peculiar, however, are the regulated upstream single-stranded elements. Why are these sites melted when c-*myc* is expressed? One possible hypothesis relates these single-stranded elements with factors binding to single-stranded DNA. Actively transcribing genes accrue positive supercoils ahead of moving transcription complexes and negative supercoils behind (39). Regions of negative superhelical tension melt more easily. Thus, transcription can have a profound effect on the conformation of chromatin and may be a driving force in the creation of single-stranded or open upstream regions, thereby facilitating the binding of single-stranded-DNA-binding factors such as FBP or hnRNP K to their cognate sequences. Support of this hypothesis came from a recent study showing that FBP imparts mung bean nuclease sensitivity within FUSE when the DNA is supercoiled but not when it is relaxed (5). If the binding of these proteins to torsionally strained DNA in vitro is biologically significant, then the in vivo and in vitro patterns of $KMnO_4$ at FUSE should be similar. To address this issue, recombinant FBP, which binds to the bottom strand of FUSE in vitro, was incubated with either linear or supercoiled plasmid DNA containing the 3.3-kb *Hin*dIII-*Sst*I genomic c-*myc* fragment (Materials and Methods). Protein-DNA mixtures were exposed to $KMnO_4$ and subjected to LMPCR. As shown in Fig. 5A, lanes 1 and 3, FBP dramatically increased the $KMnO_4$ reactivity on the top strand of a 72-nucleotide segment only in supercoiled DNA (compare lanes 3 and 5). Different lengths of exposure to $KMnO_4$ had little effect on the footprint. GST alone had no effect on the reactivity of this segment (lanes 2 and 4). The conformational changes induced by FBP in vitro were highly related to pattern features of FUSE modification seen in vivo (Fig. 5B, lanes 3 and 4). Both the margins of the single-stranded region and the profile of the reactive bases were largely equivalent, differing only by suppression of reactivity at a few bases in vivo relative to in vitro.

The lower strand of FUSE is bound by FBP in vitro and displays a mixture of protection from permanganate oxidation and hypersensitivity in vivo (Fig. 5C, lane 6). This pattern was largely recapitulated with the in vitro assay (Fig. 5C, lane 3). Three guanine residues (−1539, −1538, and −1537) within the *Ava*I recognition sequence, reactive in vitro with naked linear or supercoiled plasmid DNA but protected in vivo, were also protected in vitro by FBP but not by GST. Many of the bases reactive or protected in vivo were similarly affected in vitro by the binding of FBP. These changes are summarized in Fig. 5D. These data strongly suggest that FBP is indeed bound to the FUSE site in vivo. Although occasional $KMnO_4$-specific cleavages appeared with naked supercoiled DNA but not with linear plasmid, the vast majority of modifications were protein specific (compare lanes 1 and 2). Thus, supercoil-induced conformational changes may serve as a nidus from which FBP opens duplex DNA.

FBP has separable DNA binding domains with separate specificities. The central domain of FBP consists of four regularly spaced units, each constituted by a variant of a KH motif, followed by a short spacer and an amphipathic helix (18) (Fig. 6B). FBP units 3 and 4 (FBP_{3+4}) bind tightly to a 33-nucleotide sequence (Fig. 6B), totally enveloped within the

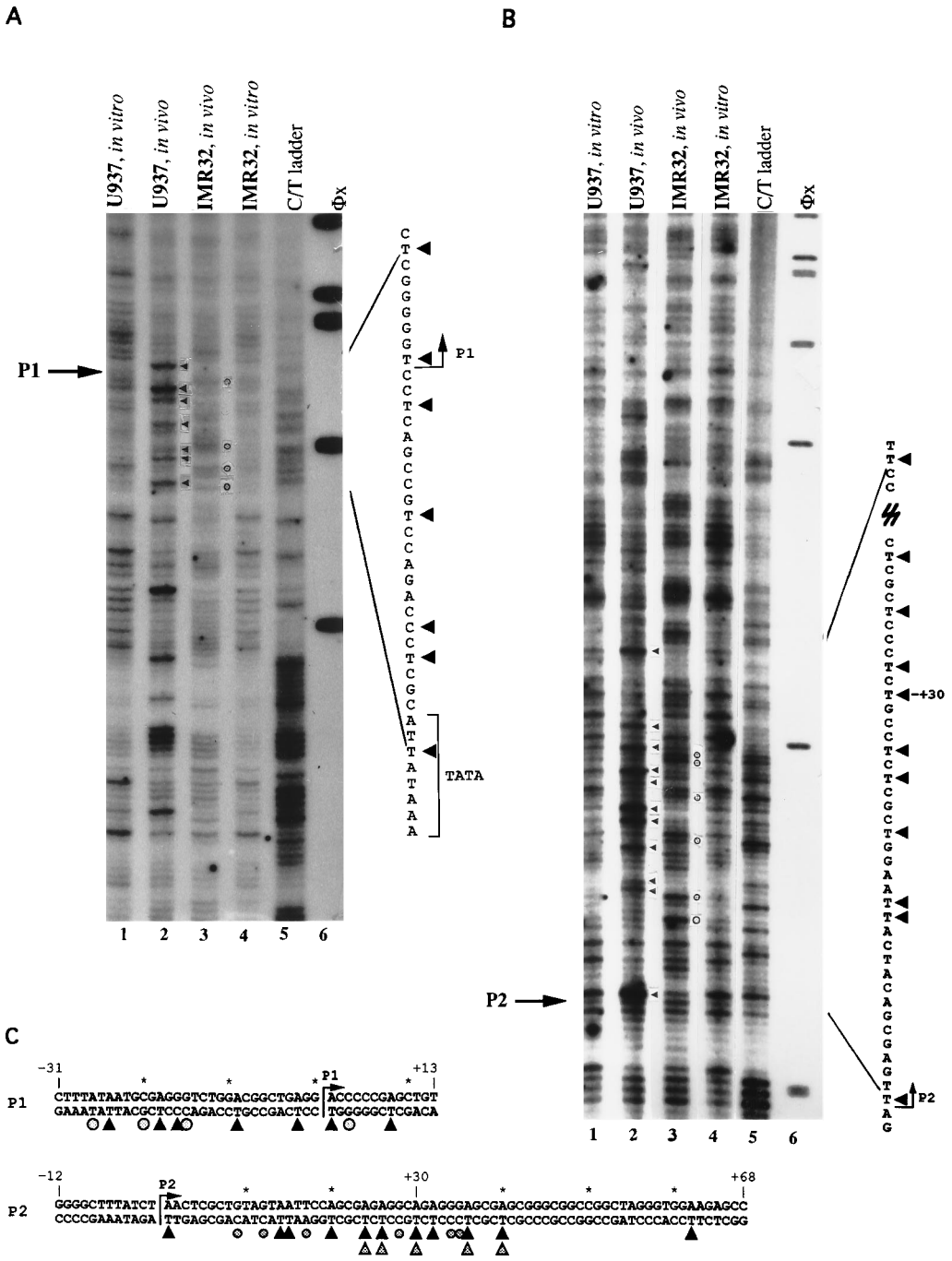

FIG. 4. Distinct conformations in expressed or silent c-*myc* at promoters P1 and P2. (A) Distinct conformation of expressed and silent c-*myc* P1 promoter bottom (template) strand in vivo. CT bottom-strand primers were used to more closely analyze $KMnO_4$ reactivity of P1. Lane designations and symbols are as in Fig. 3. Hyperreactive residues in IMR32 cells are marked by circles. (B) Distinct conformation of expressed and silent c-*myc* P2 promoter bottom (template) strand in vivo. P2 bottom-strand primers were used to more closely analyze $KMnO_4$ reactivity of P2. Lane designations are as in Fig. 3. Shaded triangles indicate the locations of $KMnO_4$ hypersensitivity described previously (37). (C) Sequence summary of $KMnO_4$ modifications at P1 and P2. Designations are as described above. Arrows indicate the start of transcription.

72-nucleotide found melted in vivo and opened by FBP in vitro. In contrast, proteins derived from FBP possessing only units 1 and 2 (FBP_{1+2}) had almost no affinity for this 33-nucleotide sequence. The larger segment of DNA rendered susceptible to chemical modification by FBP in vitro predicted FBP-DNA interactions extending upstream of the 33-nucleotide segment. Reasoning that these additional interactions might be mediated by units 1 and 2, we performed $KMnO_4$ in vitro assays with the separated DNA binding domains (FBP_{1+2} and FBP_{3+4}) as well as full-length FBP. As shown in Fig. 5B, lane 5, FBP_{3+4} generated only the most downstream hypersensitivities, relative to the full-length protein. If FBP_{3+4} bound only to the downstream portion of FUSE, were units 1 and 2 recognizing the upstream portion (Fig. 5E)? Unlike

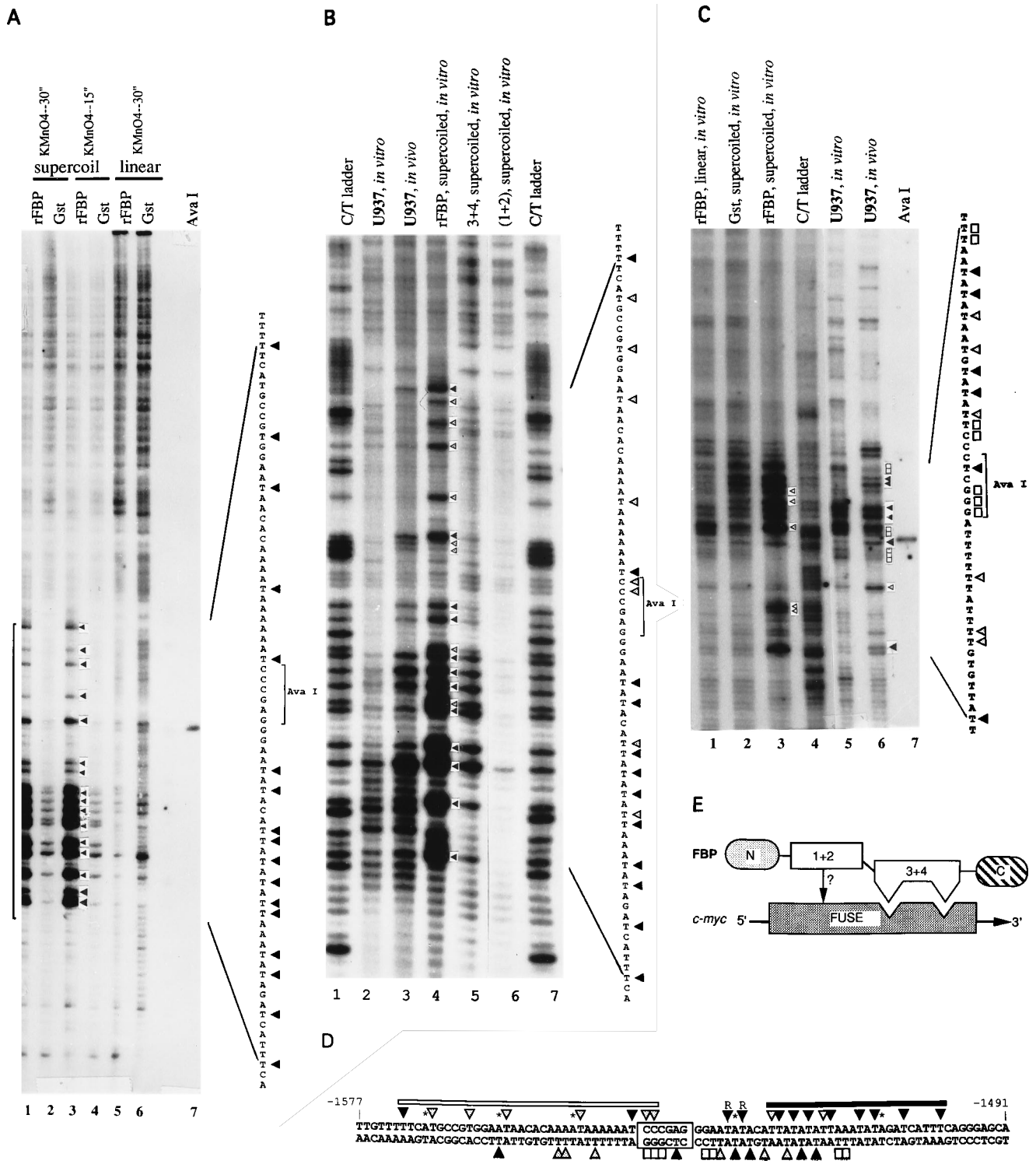

FIG. 5. FBP binds to FUSE in supercoiled but not linear DNA. (A) Recombinant GST-FBP (rFBP; 3.9 μg) or GST (0.95 μg) was incubated with either supercoiled or linear plasmid containing a 3.3-kb *Hin*dIII-*Sst*I fragment of the human c-*myc* 5′ regulatory region. Samples were then exposed to 25 mM $KMnO_4$ for 30 s on ice and subjected to piperidine treatment and LMPCR with FUSE top-strand oligonucleotides. Triangles indicate hyperreactivity present in supercoiled plasmid DNA relative to GST or linear plasmid DNA controls. (B) FBP_{3+4} opens the 3′ half of FUSE relative to full-length FBP. Equimolar amounts of full-length FBP (3.9 μg), FBP_{3+4} (2.0 μg), and FBP_{1+2} (1.9 μg) were incubated with either linear or supercoiled plasmid. U937 DNA, treated in vivo or in vitro, is included for comparison. Closed triangles indicate hyperreactivity present both in U937 chromatin and in plasmid; shaded triangles indicate hyperreactivity not shared by in vivo and in vitro samples. (C) FBP in vitro both protects and induces $KMnO_4$ cleavages at specific residues on the FUSE bottom strand, similar to what is seen in vivo. FUSE bottom-strand oligonucleotides were used to analyze the FUSE bottom strand. To facilitate comparison, reactions were run alongside U937 DNA treated in vivo or genomic DNA treated in vitro. Protections are indicated by squares. Other designations are as described above. (D) Summary of $KMnO_4$ modifications at FUSE. Designations are as described above. The *Ava*I site is boxed for reference. The solid bar indicates residues that are $KMnO_4$ reactive with FBP_{3+4} protein; the open bar indicates residues unreactive to FBP_{3+4} relative to full-length FBP; R indicates residues of reduced $KMnO_4$ reactivity with FBP_{3+4} relative to full-length FBP. (E) Schematic representation of the results in panel B showing FBP_{3+4}-induced $KMnO_4$ modifications to only the 3′ portion of FUSE, suggesting an FBP_{1+2} interaction with the 5′ portion of FUSE.

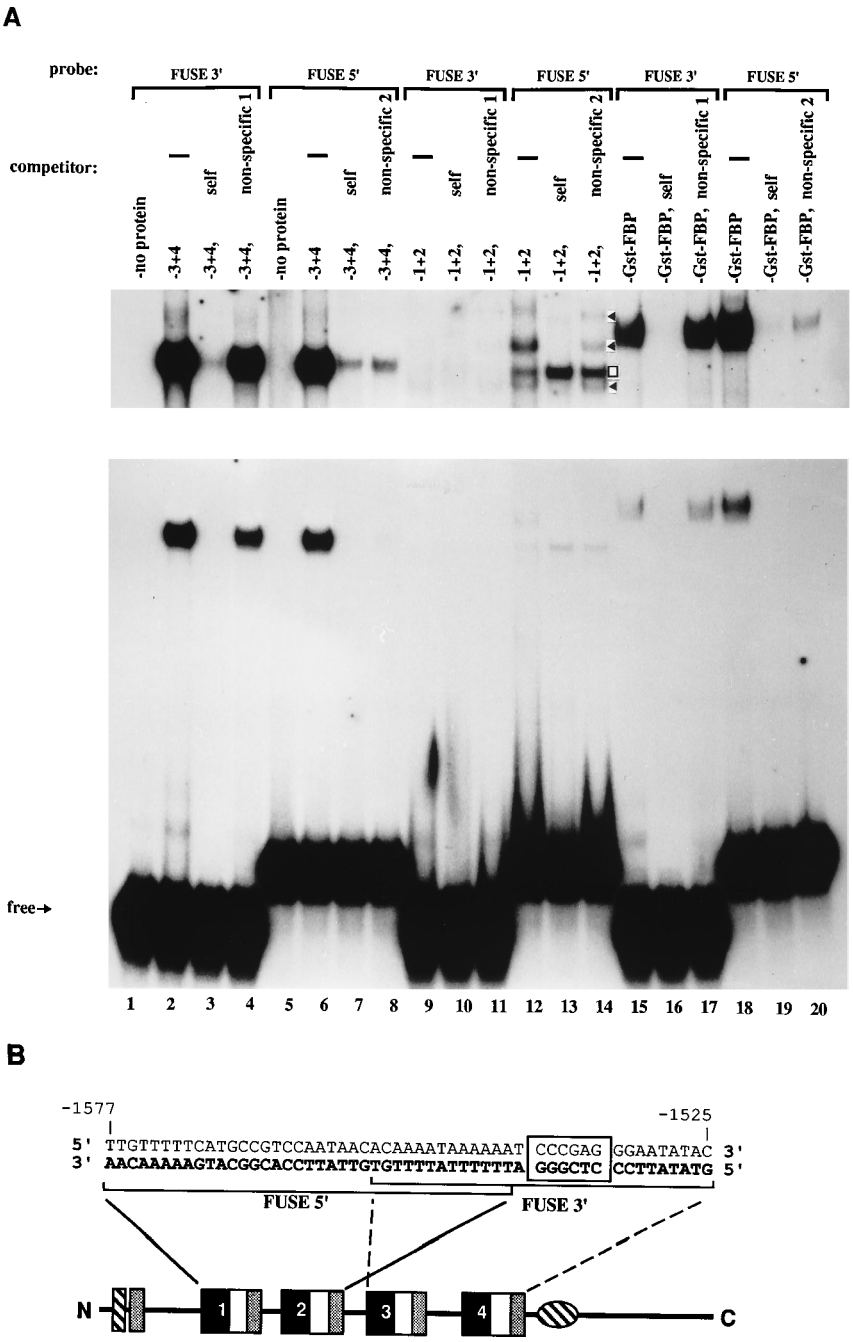

FIG. 6. FBP has separable DNA binding domains with different specificities. (A) FBP_{1+2} and FBP_{3+4} have affinities for 5′ and 3′ portions of FUSE, respectively. Recombinant GST-FBP_{3+4} (10 ng), GST-FBP_{1+2} (80 ng), and GST–full-length FBP (5 ng) fusion proteins were incubated with either the 5′ or 3′ FUSE ^{32}P-labeled oligonucleotide probe in a typical binding reaction. Proteins were incubated with probe or a combination of probe and a 200-fold molar excess of unlabeled competitor. DNA-protein complexes were separated from free probe (free) on an 8% nondenaturing polyacrylamide gel at 4°C and visualized by autoradiography. The upper portion shows a longer exposure to facilitate visualization of the specific FBP_{1+2} shifts (indicated by arrowheads). The square indicates a less specific FBP_{1+2} shift. (B) Sequences of the single-stranded oligonucleotide probes used in the electrophoretic mobility shift assay and schematic representation of FBP. Hatching indicates glycine-rich segments; solid boxes indicate FBP repeats; shaded boxes represent amphipathic helices; open boxes represent spacer regions (18). The sequences of the nonspecific oligonucleotides and preparation of the recombinant proteins are specified in Materials and Methods.

FBP_{3+4}, FBP_{1+2} could not bind to FUSE in supercoiled duplex (Fig. 5C, lane 6) because of either an inability to melt DNA or the complete absence of FUSE recognition. To distinguish between these possibilities, FBP_{1+2} and FBP_{3+4} were compared with respect to relative binding to upstream and downstream segments of FUSE bottom-strand sequence (Fig. 6B). FBP_{3+4} (as well as the full-length protein) bound specifically to the downstream 3′ 33-mer probe (Fig. 6A, lanes 2 to 4 and 15 to 17) but only nonspecifically to the upstream 5′ probe (Fig. 6A, lanes 6 to 8 and 18 to 20). Conversely, FBP_{1+2} bound specifically only to the upstream 5′ probe, not to the downstream 3′ probe (compare lanes 9 to 11 and lanes 12 to

14). However, 15-fold more FBP_{1+2} than FBP_{3+4} was required for specific complex formation, indicating that units 1 and 2 possess lower affinity for DNA (all of the DNA-protein complexes formed with FBP_{1+2} reacted with anti-GST, eliminating the possibility of weak binding to a contaminating protein [data not shown]). As expected, the full-length protein behaves as a composite of FBP_{1+2} and FBP_{3+4} (Fig. 6A, lanes 15 to 20). Thus, separable segments of FBP interact with adjacent sequences in single-stranded DNA, but native coupling between units is necessary to open and bind the full FUSE region and to generate the chemical reactivity seen in vivo in cells which express c-*myc*.

hnRNP K associates with and opens the CT element in supercoiled DNA. FBP and hnRNP K have homology in their respective DNA binding domains (termed K homology), and both proteins bind their cognate sequences as single strands in vitro (18, 63). Moreover, the c-*myc cis* elements to which these factors bind (FUSE and the CT element) display S1 hypersensitivity in vivo. Thus, if the topology and conformation of the CT element are coupled with c-*myc* transcription, then binding or release of hnRNP K might be governed by helical torsional stress and monitored by the appearance of strong $KMnO_4$ reactivity within the CT element, using parallel experiments described earlier, involving FUSE and recombinant FBP. To test this hypothesis, recombinant hnRNP K, which has been shown to bind to the top (pyrimidine-rich) strand of the CT element in vitro, was incubated with either linear or supercoiled c-*myc* DNA containing the CT element and subjected to permanganate oxidation. As shown in Fig. 7, hnRNP K creates dramatic hypersensitivities within the CT element on both the top and bottom strands, but only if the target DNA is supercoiled. Remarkably, on the top strand, the strand to which hnRNP K binds in vitro, the most prominent reactions were with the same CT element residues most sensitive to permanganate in vivo in U937 cells (Fig. 7B; compare lanes 4 and 5). CT opening was hnRNP K specific, as other proteins, including FBP (data not shown) and other single-stranded-DNA-binding proteins, did not alter the permanganate reactivity of naked DNA at this site. No hnRNP K-induced cleavages were seen on linear DNA (Fig. 7B, lane 7). Modifications are summarized in Fig. 7C.

When the top (pyrimidine-rich) strand of the CT element is bound by hnRNP K, the displaced bottom strand should be single stranded and thus sensitive to permanganate oxidation. Every thymine within and flanking the CT element was clearly reactive to permanganate in vitro (Fig. 7A, lane 4). These hypersensitivities mapped to thymines −155, −143, −134, −125, −116, −114, and −113. Of these residues, only thymidine −113 was not sensitive in vivo (Fig. 7A, lane 2). The permanganate reactions were most strong within and flanking CT repeats II and III but were still prominent in repeats IV and V. Again, no other protein generated these cleavages and hnRNP K induced no reactive bases when the target DNA was linearized (data not shown). These data strongly argue that hnRNP K is associated with the CT element in vivo.

Opening of the CT element by hnRNP K can be modulated by other proteins. Several proteins in addition to hnRNP K, including Sp1 and CNBP (15, 41), have been suggested to control CT-element activity in vivo. CNBP binds to the lower strand of the CT element and hence potentially synergizes with hnRNP K on melted DNA. As shown in Fig. 7A, lane 7, CNBP alone does not modify the permanganate reactivity of the CT element in supercoiled DNA. Thus, CNBP cannot invade duplex CT elements, nor is sufficient single-stranded character present to allow trapping of a melted segment by CNBP. However, in the presence of hnRNP K, the reactivity of the CT repeats IV and V is augmented on the lower, purine-rich strand (lane 5, thymidines −155 and −143) by the presence of CNBP. Thus, binding of hnRNP K may facilitate CNBP recognition of the purine strand of the CT element.

Sp1 is a typical zinc finger protein and recognizes duplex DNA (8). Clearly, the binding of single-strand-requiring proteins and binding of duplex-requiring proteins are mutually exclusive. Accordingly, Sp1 was used to investigate the effect of duplex stabilization on hnRNP K binding. Complexes formed in vitro between hnRNP K and CT elements in supercoiled DNA were challenged with the addition of recombinant Sp1, and DNA conformation was monitored with permanganate oxidation. As shown in Fig. 7A, lane 8, Sp1 eliminated helix opening in repeats IV and V but only partly dislodged hnRNP K from repeats I to III. CNBP thus enhanced and Sp1 inhibited opening of repeats IV and V in the presence of hnRNP K. When all three factors were mixed, the effect of Sp1 was dominant over that of CNBP, and repeats IV and V were closed (Fig. 7A, lane 3). Sp1 produced no footprint in this $KMnO_4$ assay (Fig. 7B, lane 9). Similar assays were performed with dimethyl sulfoxide as the base-modifying agent. These reactions verified that Sp1 bound to the CT element, protecting repeats IV and V (data not shown). Taken together, these results suggest that the $KMnO_4$ footprint seen in vivo may reflect a combination of Sp1, CNBP, and hnRNP K. Thus, a complex equilibrium must exist at the CT elements in vivo; alteration of the conformation of the CT element could facilitate or block the action of mutually exclusive constellations of factors, thereby allowing a single regulatory sequence to confer different properties upon nearby promoters.

DISCUSSION

Several classes of single-stranded *cis* elements occur within the c-*myc* gene in vivo. DNA segments sensitive to chemical and enzymatic probes selective for single strands are scattered throughout the c-*myc* regulatory sequence. Moreover, these melted regions colocalize with DNase I-hypersensitive sites. Although DNase I-hypersensitive sites are associated with the regulatory elements of numerous genes, the conformational basis for the hypersensitivity is not established. Thus, the utilization of conformation-sensitive probes such as $KMnO_4$ and S1 nuclease complements the use of more standard probes of protein-DNA interactions such as dimethyl sulfoxide and DNase I; features well visualized with one set of reagents are sometimes undetected by the other. For example, FBP binding to FUSE is readily detected with single-strand-selective agents, whereas Sp1 interacting with the CT element is seen only with the more conventional reactions. Just as DNase I-hypersensitive sites are heterogeneous and associated with different physiological states, so their associated single-stranded zones might prove to be diverse in origin; for example, some segments might melt constitutively, whereas the opening of others might be regulated. Some factors may directly invade duplex, while others may exploit torsional energy generated by molecules acting at distant sites. Thus, the single-stranded segments upstream of c-*myc*, detected with permanganate and S1 nuclease, may result from a variety of regulatory events.

c-*myc* promoters have at least three states. At promoters, DNA melting is obligatory. At the c-*myc* promoters P1 and P2, where transcription initiation is associated with an engaged but paused RNA polymerase, the duplex is necessarily propped open. The data presented here suggest that distinct open P1 and P2 complexes are associated with different physiological states. First, in cells expressing c-*myc* or in which c-*myc* transcription has been recently attenuated, initiated polymerases

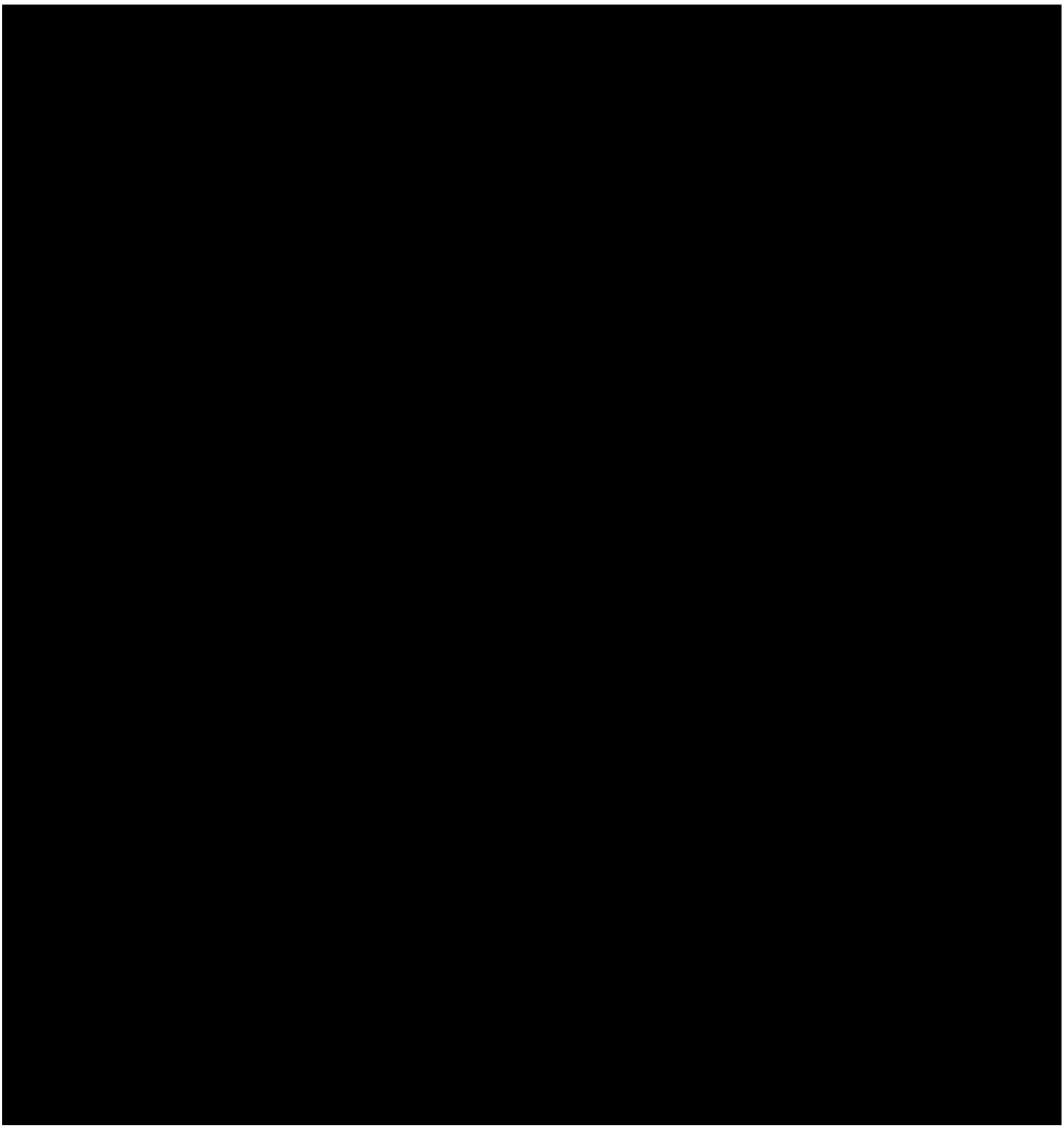

FIG. 7. hnRNP K binds to CT elements in supercoiled but not linear DNA. (A) hnRNP K opens the CT-element bottom strand in supercoiled DNA synergistically or antagonistically with other factors. Recombinant proteins were incubated singly or in equimolar amounts (hnRNP K, 1.0 μg; CNBP, 0.44 μg; Sp1, 1.0 μg) with supercoiled DNA, treated with $KMnO_4$, and analyzed by LMPCR with CT bottom-strand oligonucleotides. To facilitate comparison, reactions were run alongside U937 DNA treated in vivo or genomic DNA treated in vitro. Closed triangles designate hypersensitivities in vivo or induced by hnRNP K in vitro. Shaded triangles designate residues rendered reactive only by hnRNP K in vitro. (B) hnRNP K opens the CT-element top strand in supercoiled but not linear DNA. Recombinant hnRNP K (3.9 μg) or GST (0.95 μg) was incubated with supercoiled or linear DNA treated as described above. $KMnO_4$-induced cleavages on the top strand of the CT element were revealed by using CT top-strand oligonucleotides. Lane designations are as in panel A. (C) Sequence summary of $KMnO_4$ modifications at the CT element. Designations are as in panel A. The *Sma*I site is boxed and shown for reference.

awaiting promoter clearance render the immediate vicinity sensitive to single-strand-selective agents. As the interval fol lowing c-*myc* shutoff lengthens, the changes associated with active transcription decay and the promoters react like naked DNA (36, 37). Thus, the first two states of the c-*myc* promoters are defined by the presence or absence of assembled activatable transcription complexes at RNA start sites.

Analysis of melted DNA at the perpetually silent c-*myc* promoters neuroblastoma cells (overexpressing N-*myc*) reveals a third promoter state, open but repressed. The fine structure

of these inactive P1 and P2 promoters, revealed with permanganate oxidation, is totally incompatible with the patterns at active, attenuated, or vacant promoters. Thus, this third c-*myc* configuration possesses promoter complexes either composed of different components or fixed in distinct, inactive conformations.

FUSE is a regulated c-*myc cis* element. More unexpected than melted promoters are upstream single-stranded segments such as FUSE. Three independent sets of experiments indicate that the DNA structure of FUSE is coregulated with c-*myc* expression in vivo: (i) the regularly spaced nucleosome ladder detected with micrococcal nuclease is disrupted at FUSE in c-*myc*-expressing cells but is undisturbed in cells which cannot express *myc*; (ii) the FUSE region in nuclei from cells with active c-*myc* genes is sensitive to S1 nuclease, whereas this region is not cleaved in cells with quiescent c-*myc* loci; and (iii) hyperreactivity of FUSE with the single-strand-selective agent permanganate is absent in cells with a silent c-*myc* gene. The latter two experiments each independently support the notion that FUSE is underwound in vivo when c-*myc* is expressed. On the top strand of FUSE, only hyperreactivity with permanganate is noted, whereas both unequivocal protection and hyperreactivity are seen on the bottom strand, just as predicted if FBP is the *trans* factor acting at FUSE. FBP possesses both multiple repeats of a powerful tyrosine-rich activation motif and a potent repression domain and thus can modify c-*myc* expression directly via melted FUSE binding (19). Logically, however, at least two requirements must be fulfilled in order for FBP to function: first, FBP must be expressed, and second, FUSE must be accessible to FBP and hence be melted or torsionally strained. The second condition is not met in neuroblastoma cells, in which FUSE is clearly duplex despite the presence of FBP. As FBP cannot bind specifically to linear or relaxed duplex DNA, some process or other factor must gate access to FUSE.

The CT element is the focal point of a complex equilibrium. The FUSE element is not unique among upstream sequences with respect to its sensitivity to single-strand-selective agents and its capacity to bind single-strand- and supercoil-dependent factors. Near P1, the CT region is reactive in vivo with permanganate and hypersensitive to S1 nuclease, indicating that at least some c-*myc* genes assume unusual conformations. hnRNP K, which is related to FBP, can bind to either single-stranded or supercoiled target sequences on the top strand of the CT element. When binding to torsionally strained duplex, hnRNP K exposes sites on the bottom strand for binding with CNBP (63). Thus, factors or processes which facilitate hnRNP K binding will also augment CNBP activity. In contrast, Sp1 antagonizes the DNA-protein interactions of both hnRNP K and CNBP, the latter profoundly. Conceptually, Sp1 may modulate hnRNP K and CNBP activity through at least two mechanisms: first, through steric competition for binding at a single site, and second, by shifting the equilibrium of a larger segment from the melted to duplex state. Thus, the configuration of the CT element will be governed by the intrinsic equilibrium between single and double strands, with constraints imposed by the degree of torsional stress and the relative amounts and affinities of the relevant factors for the DNA and (potentially) for each other. Interconverting a single segment of DNA from duplex to single strands could allow one *cis* element to interact with alternate sets of *trans* factors without disturbing the balance between these same proteins at other sites as would occur if factor levels fluctuated. In this work, we have focused on a handful of single-stranded sites shown previously to bind known proteins and to behave as *cis*-acting elements altering c-*myc* expression; the variety of single-stranded *cis* elements and their associated *trans* factors may be expected to increase as the properties of melted segments are explored.

Implications of single-stranded *cis* elements and associated *trans* factors for *myc* regulation. The existence of several c-*myc* *cis* elements possessing single-stranded properties in vivo, coupled with the demonstration that some sequence-specific single-stranded-DNA-binding proteins also recognize their cognate targets in supercoiled DNA, has potentially broad implications for c-*myc* regulation and important ramifications for gene regulation in general. Studies have shown that duplex DNA is refractory to twisting over short stretches (<1,000 bp) (33). For example, if the length of a DNA fragment is an integral number of helical turns, then it can be ligated into a circle hundreds of times more efficiently than if the 5′ and 3′ ends are out of phase. Helical phasing is required for proteins to bind cooperatively to sites separated on duplex DNA (32). One potential role of single-stranded elements concerns the dramatic decrease in the torsional rigidity manifested in duplex DNA when as few as three mismatched base pairs are introduced (33). Together with a smaller decrease in flexural rigidity at these same sites, the net effect would be the creation of a single-stranded hinge, facilitating the interaction of elements and factors that might otherwise be disfavored energetically. For a gene regulated by multiple factors bound at different distances from the promoters and from each other, such a single-stranded hinge, acting over several hundred base pairs, could determine which proteins exert the predominant influence on *myc* expression at any instant.

The linkage between melting and supercoiling has regulatory ramifications. In eukaryotes, transcription is the main generator of unrestrained supercoils (restrained supercoils are created intrinsically when DNA is wrapped around nucleosome octamers, but these are necessarily inaccessible to single-stranded-DNA-binding proteins [13]). Therefore, repressed genes are less underwound than active genes. The action of transcriptional activators recognizing relaxed B-DNA is therefore demanded to activate, de novo, a previously inactive promoter and subsequently generate topological strain. Independently or in concert, different activators might serve as an ignition switch to turn on transcription, but steady-state regulation might subsequently be superimposed. In fact, some enhancers have recently been shown to function as just such a binary switch, increasing the probability that a promoter is active but not governing the rate of transcription once a gene is turned on (65). Conformation- and topology-sensitive factors such as FBP have properties well suited to function as a molecular cruise control. Once sufficient torsion exists to allow binding of strain-sensing factors, these molecules could constitute a direct, *cis*-acting monitor of promoter activity. If possessing appropriate effector domains, these factors could confer a real-time feedback regulation onto a gene. Thus, the control circuitry maintaining steady-state expression would employ components different from those used to induce initial expression. Even on linear DNA, in the absence of a fixed topological border, ongoing transcription can produce enough transient strain to alter the activity of a nearby promoter. For example, T7 RNA polymerase transcribing from a phage promoter placed upstream and divergent from an rRNA promoter can activate the rRNA promoter in *Xenopus* oocytes on linear DNA (17). This facilitation of RNA polymerase I action is further augmented by topoisomerase inhibitors, attesting to the topologic mechanism of this activation. An additional example of a well-characterized, topologically controlled mechanism was elucidated by Gralla and coworkers, who used chemical probes to identify supercoil-dependent regulation of the *lac* operon (11, 49).

Processes which alter superhelical density could modify the binding of proteins such as FBP and hnRNP K. Among these processes are conformational changes in DNA such as localized melting, hairpin extrusion, and transition to Z-DNA, each of which can serve as a reservoir for the torsional energy generated during transcription. Any interaction between proteins bound to DNA at separated sites defines and isolates a new topological domain. As demonstrated recently in minichromosomes, packing DNA into nucleosomes itself renders DNA less susceptible to the action of topoisomerases (44). Similarly, a small topologically closed domain created by the interaction of *trans*-acting factors could reduce and regulate the action of torsion-opposing topoisomerases. In addition, interactions between upstream factors and the transcription machinery could put into the loop particular elements which constrain transcription-driven torsion. Likewise, factors bound out of the loop could not be under the direct influence of transcriptionally generated supercoils. Considering the variety of protein-protein interactions between large complexes bound to DNA occurring during transcription, a large number of complex and interlocked topological configurations are likely; proteins such as FBP and hnRNP K may provide the cell with the tools to exploit non-B-DNA structures and conformations to achieve homeostasis.

ACKNOWLEDGMENTS

We thank U. Siebenlist, C. Wu, L. Liotta, and S. Mackem for critical review of the manuscript. We are grateful to L. Bazar and M. Avigan for sharing data prior to publication and to S. Sanford for excellent technical assistance.

REFERENCES

1. **Aller, P., C. Rius, F. Mata, A. Zorilla, C. Cabanas, T. Bellon, and C. Bernabeu.** 1992. Camptothecin induces differentiation and stimulates the expression of differentiation-related genes in U937 human promonocytic leukemia cells. Cancer Res. **52:**1245–1251.
2. **Ausubel, F. M., R. Brent, R. E. Kingston, D. D. Moore, J. G. Seidman, and J. A. Smith (ed.).** 1989. Current protocols in molecular biology. John Wiley & Sons, New York.
3. **Avigan, M. I., B. Strober, and D. Levens.** 1990. A far upstream element stimulates c-*myc* expression in undifferentiated leukemia cells. J. Biol. Chem. **265:**18538–18545.
4. **Battey, J., C. Moulding, R. Taub, W. Murphy, T. Stewart, H. Potter, G. Lenoir, and P. Leder.** 1983. The human c-*myc* oncogene: structural consequences of translocation into the IgH locus in Burkitt lymphoma. Cell **4:**779–787.
5. **Bazar, L., D. Meighen, V. Harris, R. Duncan, D. Levens, and M. Avigan.** 1995. Targeted melting and binding of a DNA regulatory element by a transactivator of *c-myc*. J. Biol. Chem. **270:**8241–8248.
6. **Bentley, D. L., and M. Groudine.** 1986. A block to elongation is largely responsible for decreased transcription of *c-myc* in differentiated HL60 cells. Nature (London) **321:**702–706.
7. **Bentley, D. L., and M. Groudine.** 1986. Novel promoter upstream of the human c-*myc* gene and regulation of c-*myc* expression in B-cell lymphomas. Mol. Cell. Biol. **6:**3481–3489.
8. **Berg, J. M.** 1992. Sp1 and the subfamily of zinc finger proteins with guanine-rich binding sites. Proc. Natl. Acad. Sci. USA **89:**11109–11110.
9. **Bergemann, A. D., and E. M. Johnson.** 1992. The HeLa Pur factor binds single-stranded DNA at a specific element conserved in gene flanking regions and origins of DNA replication. Mol. Cell. Biol. **12:**1257–1265.
10. **Bergemann, A. D., Z.-W. Ma, and E. M. Johnson.** 1992. Sequence of cDNA comprising the human *pur* gene and properties of the encoded protein. Mol. Cell. Biol. **12:**5673–5682.
11. **Borowiec, J. A., L. Zhang, S. Sasse-Dwight, and J. D. Gralla.** 1987. DNA supercoil promoter formation of a bent repressor loop in *lac* DNA. J. Mol. Biol. **196:**101–111.
12. **Bossone, S., C. Asselin, A. Patel, and K. Marcu.** 1992. MAZ, a zinc finger protein, binds to *c-myc* and C2 gene sequences regulating transcriptional initiation and termination. Proc. Natl. Acad. Sci. USA **89:**7452–7456.
13. **Cozzarelli, N. R., and J. C. Wang.** 1990. DNA topology and its biological effects. Cold Spring Harbor Laboratory, Cold Spring Harbor Press, N.Y.
14. **Dayn, A., S. Malkhosyan, and S. M. Mirkin.** 1992. Transcriptionally driven cruciform formation *in vivo*. Nucleic Acids Res. **20:**5991–5997.
15. **DesJardins, E., and N. Hay.** 1993. Repeated CT-elements bound by zinc finger proteins control the absolute and relative activities of the two principal human c-*myc* promoters. Mol. Cell. Biol. **13:**5710–5724.
16. **Dony, C., M. Kessel, and P. Gruss.** 1985. Post-transcriptional control of *myc* and p53 expression during differentiation of the embryonal carcinoma cell line F9. Nature (London) **317:**636–639.
17. **Dunaway, M., and E. Ostrander.** 1993. Local domains of supercoiling activate a eukaryotic promoter *in vivo*. Nature (London) **361:**746–748.
18. **Duncan, R. D., L. Bazar, G. Michelotti, T. Tomonaga, H. Krutzsch, M. Avigan, and D. Levens.** 1994. A sequence-specific, single strand binding protein activates the far upstream of *c-myc* and defines a new DNA binding motif. Genes Dev. **8:**465–480.
19. **Duncan, R., I. Collins, T. Tomonaga, T. Zheng, and D. Levens.** 1996. A unique transactivation sequence motif is found in the carboxyl-terminal domain of the single-strand-binding protein FBP. Mol. Cell. Biol. **16:**2274–2282.
20. **Duyao, M., A. Buckler, and G. Sonenshein.** 1990. Interaction of an NF-kappa B-like factor with a site upstream of the *c-myc* promoter. Proc. Natl. Acad. Sci. USA **87:**4727–4731.
21. **Dyson, P., T. Littlewood, A. Forster, and T. H. Rabbitts.** 1985. Chromatin structure of transcriptionally active and inactive human *c-myc* alleles. EMBO J. **4:**2885–2891.
22. **Dyson, P., and T. H. Rabbitts.** 1985. Chromatin structure of the *c-myc* gene in Burkitt lymphomas with upstream and downstream translocation points. Proc. Natl. Acad. Sci. USA **82:**1984–1988.
23. **Eick, D., and G. W. Bornkamm.** 1986. Transcriptional arrest within the first exon is a fast control mechanism in *c-myc* gene expression. Nucleic Acids Res. **14:**8331–8346.
24. **Freeman, L. A., and W. T. Garrard.** 1992. DNA supercoiling in chromatin structure and gene expression. Crit. Rev. Eukaryotic Gene Expression **2:**165–209.
25. **Fukuchi, K., S. Tomoyasu, K. Watanabe, H. Suzuki, T. Kaetsu, Y. Takagi, N. Tsuruoka, and K. Gomi.** 1991. Increased expression of the proto-oncogene, *c-myc*, in human neuroblastoma cells by reversible inhibition of cell growth. Anticancer Res. **11:**1967–1973.
26. **Garrity, P. A., and B. J. Wold.** 1992. Effects of different DNA polymerases in ligation-mediated PCR: enhanced genomic sequencing and *in vivo* footprinting. Proc. Natl. Acad. Sci. USA **89:**1021–1025.
27. **Gazin, C., S. Dupont de Dinechin, A. Hampe, J. M. Masson, P. Martin, D. Stehelin, and F. Galibert.** 1984. Nucleotide sequence of the human *c-myc* locus: provocative open reading frame within the first exon. EMBO J. **3:**383–387.
28. **Giardina, C., and J. T. Lis.** 1995. Dynamic protein-DNA architecture of a yeast heat shock promoter. Mol. Cell. Biol. **15:**2737–2744.
29. **Giardina, C., M. Perez-Riba, and J. T. Lis.** 1992. Promoter melting and TFIID complexes on Drosophila genes *in vivo*. Genes Dev. **6:**2190–2200.
30. **Grosso, L. E., and H. C. Pitot.** 1985. Transcriptional regulation of *c-myc* during chemically induced differentiation of HL-60 cultures. Cancer Res. **45:**847–850.
31. **Hiebert, S. W., M. Lipp, and J. R. Nevins.** 1989. E1A-dependent transactivation of the human *c-myc* promoter is mediated by the E2F factor. Proc. Natl. Acad. Sci. USA **86:**3594–3598.
32. **Hochschild, A., and M. Ptashne.** 1986. Cooperative binding of λ repressors to sites separated by integral turns of the DNA helix. Cell **44:**681–687.
33. **Kahn, J., E. Yun, and D. Crothers.** 1994. Detection of localized DNA flexibility. Nature (London) **368:**163–166.
34. **Kelly, K., and U. Siebenlist.** 1986. The regulation and expression of *c-myc* in normal and malignant cells. Annu. Rev. Immunol. **4:**317–338.
35. **Kohl, N. E., N. Kanda, R. R. Schreck, G. Bruns, S. A. Latt, F. Gilbert, and F. W. Alt.** 1983. Transposition and amplification of oncogene-related sequences in human neuroblastomas. Cell **35:**359–367.
36. **Krumm, A., L. Hickey, and M. Groudine.** 1995. Promoter-proximal pausing of RNA polymerase II defines a general rate-limiting step after transcription initiation. Genes Dev. **9:**559–572.
37. **Krumm, A., T. Meulia, M. Brunvand, and M. Groudine.** 1992. The block to transcriptional elongation within the human *c-myc* gene is determined in the promoter-proximal region. Genes Dev. **6:**2201–2213.
38. **Larsen, A., and H. Weintraub.** 1982. An altered DNA conformation detected by S1 nuclease occurs at specific regions in active chick globin chromatin. Cell **29:**609–622.
39. **Liu, L. F., and J. C. Wang.** 1987. Supercoiling of the DNA template during transcription. Proc. Natl. Acad. Sci. USA **84:**7024–7027.
40. **Marcu, K. B., S. A. Bossone, and A. J. Patel.** 1992. *myc* function and regulation. Annu. Rev. Biochem. **61:**809–860.
41. **Michelotti, E., T. Tomonaga, H. Krutzsch, and D. Levens.** 1995. Cellular nucleic acid binding protein regulates the CT-element of the human *c-myc* protooncogene. J. Biol. Chem. **270:**9494–9499.
42. **Negishi, Y., Y. Nishita, Y. Saegusa, I. Kakizaki, I. Galli, F. Kihara, K. Tamai, N. Miyajima, S. Iguchi-Ariga, and H. Ariga.** 1994. Identification and cDNA cloning of single stranded DNA binding proteins that interact with the region upstream of the human *c-myc* gene. Oncogene **9:**1133–1143.
43. **Nielsen, P. E.** 1990. Chemical and photochemical probing of DNA complexes. J. Mol. Recognit. **3:**1–25.

44. **Ramsperger, U., and H. Stahl.** 1995. Unwinding of chromatin by the SV40 large T antigen DNA helicase. EMBO J. **14:**3215–3225.
45. **Riggs, K., S. Saleque, K.-K. Wong, K. Merrell, J. S. Lee, Y. Shi, and K. Calame.** 1993. Yin-yang 1 activates the c-*myc* promoter. Mol. Cell. Biol. **13:**7487–7495.
46. **Riou, J.-F., D. Lefevre, and G. Riou.** 1989. Stimulation of the topoisomerase II induced cleavage sites in the *c-myc* protooncogene by antitumor drugs is associated with gene expression. Biochemistry **28:**9104–9110.
47. **Rubin, C. M., and C. W. Schmid.** 1980. Pyrimidine-specific reactions useful for DNA sequencing. Nucleic Acids Res. **8:**4613–4619.
48. **Sambrook, J., E. F. Fritsch, and T. Maniatis.** 1989. Molecular cloning: a laboratory manual, 2nd ed. Cold Spring Harbor Laboratory Press, Cold Spring Harbor, N.Y.
49. **Sasse-Dwight, S., and J. D. Gralla.** 1988. Probing cooperative binding *in vivo*—the *lac* O_1:O_3 interaction. J. Mol. Biol. **202:**107–119.
50. **Sasse-Dwight, S., and J. D. Gralla.** 1991. Footprinting protein:DNA complexes *in vivo*. Methods Enzymol. **208:**146–168.
51. **Schubach, W., and M. Groudine.** 1984. Alteration of *c-myc* chromatin structure by avian leukosis virus integration. Nature (London) **307:**702–708.
52. **Shi, Y., J. Glynn, L. Guilbert, T. Cotter, R. Bissonnette, and D. Green.** 1992. Role for *c-myc* in activation-induced apoptotic cell death in T cell hybridomas. Science **257:**212–214.
53. **Siebenlist, U., P. Bressler, and K. Kelly.** 1988. Two distinct mechanisms of transcriptional control operate on c-*myc* during differentiation of HL60 cells. Mol. Cell. Biol. **8:**867–874.
54. **Siebenlist, U., L. Hennighausen, J. Battey, and P. Leder.** 1984. Chromatin structure and protein binding in the putative regulatory region of the *c-myc* gene in Burkitt lymphoma. Cell **37:**381–391.
55. **Skerka, C., P. Zipfel, and U. Siebenlist.** 1993. Two regulatory domains are required for downregulation of *c-myc* transcription in differentiating U937 cells. Oncogene **8:**2135–2143.
56. **Spencer, C. A., and M. Groudine.** 1991. Control of *c-myc* regulation in normal and neoplastic cells. Adv. Cancer Res. **56:**1–48.
57. **Spencer, C. A., R. LeStrange, W. Hayward, U. Novak, and M. Groudine.** 1990. The block transcription elongation is promoter dependent in normal and Burkitt's lymphoma *c-myc* alleles. Genes Dev. **4:**75–88.
58. **Strobl, L. J., and D. Eick.** 1992. Hold back of RNA polymerase II at the transcription start site mediates downregulation of *c-myc in vivo*. EMBO J. **11:**3307–3314.
59. **Strobl, L. J., F. Kohlhuber, J. Mautner, A. Polack, and D. Eick.** 1993. Absence of a paused transcription complex from the P2-promoter of a translocated *c-myc* gene in Burkitt's lymphoma cells: implication for the *c-myc* P1/P2 promoter shift. Oncogene **8:**1437–1447.
60. **Takai, T., Y. Nishita, S. Iguchi-Ariga, and H. Ariga.** 1994. Molecular cloning of MSSP-2, a *c-myc* gene single-strand binding protein: characterization of binding specificity and DNA replication activity. Nucleic Acids Res. **22:**5576–5581.
61. **Takimoto, M., J. Quinn, R. Farina, L. Staudt, and D. Levens.** 1989. Fos/jun and octamer-binding protein interact with a common site in a negative element of the human *c-myc* gene. J. Biol. Chem. **264:**8992–8999.
62. **Takimoto, M., T. Tomonaga, M. Matunis, M. Avigan, H. Krutsch, G. Dreyfuss, and D. Levens.** 1993. Specific binding of heterogeneous ribonucleoprotein particle protein K to the human *c-myc* promoter, *in vitro*. J. Biol. Chem. **268:**18249–18258.
63. **Tomonaga, T., and D. Levens.** 1995. Heterogeneous nuclear ribonucleoprotein K is a DNA binding transactivator. J. Biol. Chem. **270:**4875–4881.
64. **Vassilev, L., and E. M. Johnson.** 1990. An initiation zone of chromosomal DNA replication located upstream of the c-*myc* gene in proliferating HeLa cells. Mol. Cell. Biol. **10:**4899–4904.
65. **Walters, M. C., S. Fiering, J. Eidemiller, W. Magis, M. Groudine, and D. I. K. Martin.** 1995. Enhancers increase the probability but not the level of gene expression. Proc. Natl. Acad. Sci. USA **92:**7125–7129.
66. **Watanabe, T., E. Sariban, T. Mitchell, and D. Kufe.** 1985. Human *c-myc* and N-ras expression during induction of HL-60 cellular differentiation. Biochem. Biophys. Res. Commun. **126:**999–1005.
67. **Wittig, B., S. Wolfl, T. Dorbic, W. Vahrson, and A. Rich.** 1992. Transcription of human *c-myc* in permeabilized nuclei is associated with formation of Z-DNA in three discrete regions of the gene. EMBO J. **11:**4653–4663.
68. **Wolf, D. A., L. J. Srobl, A. Pullner, and D. Eick.** 1995. Variable pause positions of RNA polymerase II lie proximal to the *c-myc* promoter, irrespective of transcriptional activity. Nucleic Acids Res. **23:**3373–3379.
69. **Wu, C.** 1980. The 5′ ends of Drosophila heat shock genes in chromatin are hypersensitive to DNase I. Nature (London) **286:**854–860.
70. **Zhang, X., N. Jabrane-Ferrat, C. Asiedu, S. Samac, B. Peterlin, and M. Ehrlich.** 1993. The major histocompatibility complex class II promoter-binding protein RFX (NF-X) is a methylated DNA-binding protein. Mol. Cell. Biol. **13:**6810–6818.